Reprinted from The Journal of Physical Chemistry, 1982, 86, 622.
Copyright © 1982 by the American Chemical Society and reprinted by permission of the copyright owner.

Theory of Highly Exothermic Electron Transfer Reactions†

R. A. Marcus* and Paul Siders

Arthur Amos Noyes Laboratory of Chemical Physics,‡ California Institute of Technology, Pasadena, California 91125
(Received: August 6, 1981; In Final Form: October 21, 1981)

The theory of highly exothermic homogeneous outer-sphere electron transfer reactions is discussed for transfers occurring over a range of distances. A finite rate of diffusion of reactants and their long-range force are treated by solving the diffusion equation numerically for the reactant pair distribution function. Steady-state solutions for the bimolecular rate constant are compared with experimental data as well as with our recent approximate analytic solution, which is found to agree in the present case. On the basis of short-time solutions, it is proposed that experiments which measure electron transfer rates at short times following the onset of reaction improve the possibility of observing the inverted effect in bimolecular systems. The chance of seeing it in linked systems (unimolecular reactions) is even greater. The relation between the prediction of an "inverted region" in the rate constant vs. ΔG° plot and the existence of a maximum in charge transfer spectral plots of intensity vs. absorption frequency is pointed out.

Introduction

It has been predicted that the rate constant of a series of homogeneous electron transfer reactions

$$ox_1 + red_2 \rightarrow red_1 + ox_2 \qquad (1)$$

in which ox_1 or red_2 is varied (at constant intrinsic reorganization energy λ) should first increase with increasingly negative standard free energy of reaction ΔG^0 at small ΔG^0. It should then achieve a maximum at some value of ΔG^0 and thereafter decline as ΔG^0 continues to become still more negative. The region of decline was termed the "inverted" region.[1] The existence of an inverted region was first predicted on the basis of a classical theory.[1,2] The quantum-mechanical correction given by quantum-mechanical perturbation theories predicts a smaller but nevertheless finite inversion.[3-7] The difference arises from nuclear tunneling.

The experimental evidence for the existence of an inverted region is sparse: Some evidence for the effect is available for the reactions of electrons with different solutes, where the ΔG^0 for a given solute was varied by varying the hydrocarbon solvent and, thereby, the electron–solvent binding energy.[8-10] Supporting data appear in the reactions of micelle-trapped pyrene with various anion radicals,[11,12] in reactions of hydrated electrons with organic molecules trapped in micelles,[12,13] and (a small decrease) in the reduction of electronically excited bipyridyl complexes of Ru(II) by various metal bipyridyl complexes.[14,15] In the two micellar examples, the ΔG^0's are uncertain, however. Evidence has also been offered in studies[16] of the rate of fluorescence quenching of trapped electrons in a glass at 77 K by various aromatic acceptors. (To see the effect, it has been suggested,[17] it is necessary to divide the acceptors studied in ref 16 into subgroups.)

Again, according to the theoretical expressions there is a 1:1 correspondence[4] between the optical line shape and the activation rate constant k_{act} vs. the energy of reaction ΔE plot (for a weak overlap system). Thus, for a given ΔS^0, there should be a correspondence with a k_{act} vs. ΔG^0 plot for an electron transfer reaction. We then argue in a concluding section that the existence of a well-known maximum in a charge-transfer absorption vs. wavelength plot implies that there should be a maximum in the ln k_{act} vs. ΔG^0 plot.

On the other hand, many studies of highly exothermic reactions have found a diffusion-limited rate constant which extends to quite negative ΔG^0's, rather than the predicted declining rate constant, e.g., ref 18–24. (Many other examples that are sometimes cited have not been studied at sufficiently negative ΔG^0 to draw any conclusions.) These studies frequently involve measuring the rate of quenching of fluorescence by a series of reactants, where quenching was presumed or demonstrated to proceed by electron transfer. In most cases, the reason for the absence of decrease in the rate is unknown, although several possibilities have been suggested. They include (i) competing mechanisms at large $-\Delta G^0$, such as H-atom transfer,[7,25]

† This article is dedicated to Simon Bauer on his 70th birthday.
‡ Contribution No. 6502.

(1) R. A. Marcus, *Discuss. Faraday Soc.*, 29, 21 (1960).
(2) R. A. Marcus, *J. Chem. Phys.*, 43, 2654 (1965).
(3) R. P. Van Duyne and S. F. Fischer, *Chem. Phys.*, 5, 183 (1974).
(4) J. Ulstrup and J. Jortner, *J. Chem. Phys.*, 63, 4358 (1975).
(5) N. Kestner, J. Logan, and J. Jortner, *J. Phys. Chem.*, 78, 2148 (1974).
(6) R. A. Marcus in "Third International Symposium on Oxidases and Related Oxidation–Reduction Systems", T. E. King, H. S. Mason, and M. Morrison, Eds., Pergamon Press, New York, 1981.
(7) P. Siders and R. A. Marcus, *J. Am. Chem. Soc.*, 103, 748 (1981).
(8) A. O. Allen, T. E. Gangwer, and R. A. Holroyd, *J. Phys. Chem.*, 79, 25 (1975).
(9) A. Henglein, *Can. J. Chem.*, 55, 2112 (1977).
(10) S. Lipsky, *J. Chem. Educ.*, 58, 93 (1981).
(11) A. J. Frank, M. Grätzel, A. Henglein, and E. Janata, *Ber. Bunsenges. Phys. Chem.*, 80, 294 (1976).
(12) J. Ulstrup, "Charge Transfer Processes in Condensed Media, Lecture Notes in Chemistry, No. 10", Springer-Verlag, New York, 1979, pp 163–4.
(13) A. J. Frank, M. Grätzel, A. Henglein, and E. Janata, *Ber. Bunsenges. Phys. Chem.*, 80, 547 (1976).
(14) C. Creutz and N. Sutin, *J. Am. Chem. Soc.*, 99, 241 (1977).
(15) B. Brunschwig and N. Sutin, *J. Am. Chem. Soc.*, 100, 7568 (1978).
(16) J. V. Beitz and J. R. Miller, *J. Chem. Phys.*, 71, 4579 (1979).
(17) J. R. Miller, private communication.
(18) D. Rehm and A. Weller, *Isr. J. Chem.*, 8, 259 (1970).
(19) L. V. Romashov, Yu. I. Kiryukhin, and Kh. S. Bagdasar'yan, *Dokl. Phys. Chem. (Engl. Transl.)*, 230, 961 (1976).
(20) R. Scheerer and M. Grätzel, *J. Am. Chem. Soc.*, 99, 865 (1977).
(21) R. Ballardini, G. Varani, M. T. Indelli, F. Scandola, and V. Balzani, *J. Am. Chem. Soc.*, 100, 7219 (1978).
(22) V. Balzani, F. Bolletta, M. T. Gandolfi, and M. Maestri, *Top. Curr. Chem.*, 75, 1 (1978).
(23) J. Eriksen and C. S. Foote, *J. Phys. Chem.*, 82, 2659 (1978).
(24) E. Vogelmann, S. Schreiner, W. Rauscher, and H. E. A. Kramer, *Z. Phys. Chem. (Frankfurt am Main)*, 101, 321 (1976).
(25) R. A. Marcus, *Int. J. Chem. Kinet.*, 13, 865 (1981).

formation of products in excited electronic states,[7,16] or, when reaction is observed by quenching of fluorescence, exciplex formation,[26,27] (ii) quantum effects[3-7,28-31] (nuclear tunneling), (iii) a modifying effect of electron transfer occurring over a range of distances r,[25] and (iv) the increase of the reorganization parameter λ with r in case iii, thereby reducing the extent of inversion.

In the present paper we report calculations which incorporate effects ii–iv and, in part, i and compare with the experimental results of Creutz and Sutin[14] and with a simple approximation[25] to the problem. It is also proposed that experiments conducted at very short times following the onset of reaction will enhance the chances of observing inverted behavior that, in bimolecular systems, is masked by diffusion in conventional steady-state rate measurements. Unimolecular systems, in which the reactants are linked to each other, should be even better in this respect, since they are unaffected by diffusion. A brief summary of the present study has been given elsewhere.[32]

Theory

Diffusion. In extracting the "activation rate constant" from an observed rate constant that is near the diffusion limit, it can be shown that the observed rate equals the harmonic mean of the activated rate and the diffusion-limited rate, when reaction occurs at some specified encounter distance σ[33,34]

$$k_{obsd} = 1/(1/k_{act} + 1/k_{diff}) \tag{2}$$

where the diffusion rate constant k_{diff} is given by [33-35]

$$k_{diff} = 4\pi D/\int_{\sigma}^{\infty} \exp(U/k_B T) r^{-2}\, dr \tag{3}$$

In eq 3 D is the sum of the reactants' diffusion coefficients, $U(r)$ is the intermolecular potential of the reactants, and k_B is Boltzmann's constant.

Electron transfers can occur over a range of reactant separation distances, rather than only at a specified distance. In such cases the observed bimolecular rate constant k_{obsd} is related to the unimolecular rate constant $k(r)$, the rate of reaction of pairs of reactants having fixed internuclear, center-to-center, separation distance r, via a pair distribution function $g(r)$:

$$k_{obsd} = 4\pi \int_0^{\infty} g(r)\, k(r) r^2\, dr \tag{4}$$

(cf. use of eq 4 for related processes[36,37]). In eq 4 we have assumed that k and g are radially symmetric. When the system has a $k(r)$ instead of only a k at $r = \sigma$, k_{act} is defined by using eq 4 with $g(r)$ replaced by its equilibrium value, $\exp[-U(r)/k_B T]$, for $r > \sigma$ and, in the present model, by zero for $r < \sigma$, since k_{act} would be the observed rate constant if diffusion were infinitely fast. Thus

$$k_{act} = 4\pi \int_{\sigma}^{\infty} k(r) r^2 \exp(-U/k_B T)\, dr \tag{5}$$

We shall wish to compare eq 4 with the use of eq 2, 3, and 5, for reactions occurring over a range of separation distances. To this end we solve eq 6 below.

In the present case the reactants are substantially larger than the solvent molecules and so we shall assume that short-range intermolecular contributions to $g(r)$ can be neglected. Then $g(r)$ in eq 4 may be obtained as the solution to a diffusion equation,[37-39] which is given by eq 6 for the case of radial symmetry.

$$\frac{\partial}{\partial t} g(r,t) = \frac{D}{r^2}\frac{\partial}{\partial r}\left(r^2 \frac{\partial g}{\partial r}\right) + \frac{D}{k_B T r^2}\frac{\partial}{\partial r}\left(r^2 g \frac{dU}{dr}\right) - gk(r) \tag{6}$$

The first term on the right arises from the diffusive flux, the second term from the conductive flux due to the long-range intermolecular potential $U(r)$ between the reactants, and the third term from the loss of reactants due to reaction. A discussion of shortcomings of eq 6 at higher concentrations of reactants is given in ref 34 and 36.

For two reactants having charges $z_1 e$ and $z_2 e$, e being the electronic charge, U in the Debye–Hückel approximation is given by eq 7,[35,40-43] where a is the distance of closest

$$U(r) = \frac{z_1 z_2 e^2}{2\epsilon r}\left[\frac{\exp \kappa a_1}{1 + \kappa a_1} + \frac{\exp \kappa a_2}{1 + \kappa a_2}\right] \exp(-\kappa r) \tag{7}$$

approach and r is the separation distance of the two centers. In eq 7, ϵ is the static dielectric constant of the solvent, κ is the inverse of the Debye–Hückel screening length, and a_i is the radius of ion i, r_i, plus that of the principal ions of opposite sign in the ion atmosphere, r_i^a.

$$a_i = r_i + r_i^a \tag{8}$$

We comment briefly in Appendix A on some assumptions underlying eq 7. Examples of eq 7 in the literature are many and include the case[41] where $r_1 = r_2 = r_1^a = r_2^a$, the case[35,42a] (tacitly) where $r_i^a \simeq 0$, and the case where $z_1 = \pm z_2$ and higher-order corrections to eq 7 are included.[42b] The related case of colloid particles, also including additional terms, has been treated by Levine and Dube.[43] In the present paper the two reacting ions are of the same size and are both positively charged, and so $a_1 = a_2 \equiv a$, i.e.

$$U(r) = \frac{z_1 z_2 e^2}{\epsilon r}\frac{\exp \kappa a}{1 + \kappa a} \exp(-\kappa r) \tag{9}$$

and a is the distance of closest approach between a reacting ion and the principal ion of opposite sign in the ion atmosphere.

At large internuclear separations, the concentration of reactants must equal the bulk (no reaction) concentration. Thus, one of the boundary conditions on eq 6 is $\lim g(r,t) = 1$ as $r \to \infty$. When a volume distributed rate constant $k(r)$ is used instead of the usual surface one $k(\sigma)$, the boundary condition at the distance of closest approach $r = \sigma$ is obtained by requiring total flux (diffusive plus conductive) across $r = \sigma$ to be zero. This inward-directed

(26) A. Weller and K. Zachariasse, *Chem. Phys. Lett.*, 10, 590 (1971).
(27) J. Jousset-Dubien, A. C. Albrecht, H. Gerischer, R. S. Knox, R. A. Marcus, M. Schott, A. Weller, and F. Willig, *Life Sci. Res. Rep.*, 12, 129 (1979).
(28) R. A. Marcus and N. Sutin, *Inorg. Chem.*, 14, 213 (1975).
(29) R. R. Dogonadze, A. M. Kuznetsov, and M. A. Vorotyntsev, *Z. Phys. Chem. (Wiesbaden)*, 100, 1 (1976).
(30) S. Efrima and M. Bixon, *Chem. Phys. Lett.*, 25, 34 (1974); *Chem. Phys.*, 13, 447 (1976).
(31) W. Schmickler, *J. Chem. Soc., Faraday Trans. 2*, 72, 307 (1976).
(32) R. A. Marcus and P. Siders, *Adv. Chem. Soc.*, in press.
(33) R. A. Marcus, *Discuss. Faraday Soc.*, 29, 129 (1960).
(34) R. M. Noyes, *Prog. React. Kinet.*, 1, 129 (1961).
(35) P. Debye, *Trans. Electrochem. Soc.*, 82, 265 (1942).
(36) J. Keizer, *J. Phys. Chem.*, 85, 940 (1981).
(37) M. J. Pilling and S. A. Rice, *J. Chem. Soc., Faraday Trans. 2*, 71, 1563 (1975); P. R. Butler, M. J. Pilling, S. A. Rice, and T. J. Stone, *Can. J. Chem.*, 55, 2124 (1977).
(38) T. R. Waite, *J. Chem. Phys.*, 28, 103 (1958).
(39) G. Wilemski and M. Fixman, *J. Chem. Phys.*, 58, 4009 (1973).
(40) We are indebted to Dr. Norman Sutin for calling to our attention the variety of work term expressions currently used in the literature and for noting several inconsistencies among them.
(41) P. Debye and E. Hückel, *Phys. Z.*, 24, 185 (1923).
(42) (a) W. J. Moore, "Physical Chemistry", 4th ed., Prentice-Hall, Englewood Cliffs, NJ, 1972, Chapter 10, for the case $a_1 = a_2$; S. Wherland and H. B. Gray, *Proc. Natl. Acad. Sci. U.S.A.*, 73, 2950 (1976); (b) G. Scatchard and J. G. Kirkwood, *Phys. Z.*, 33, 297 (1932).
(43) S. Levine and G. P. Dube, *Trans. Faraday Soc.*, 35, 1125 (1939); G. P. Dube and S. Levine, *ibid.*, 35, 1141 (1939).

flux (per unit concentration) is given by $4\pi r^2 D$ times the left-hand side of

$$\frac{\partial}{\partial r}g(r,t) + g\frac{dU}{dr}\Big/(k_BT) = 0 \qquad \text{at } r = \sigma\ (t \geq 0) \qquad (10)$$

and so eq 10 provides the second boundary condition.

A derivation of eq 2, 3, and 5, as an approximate solution to eq 6 and 10 at steady-state, is given in Appendix B.

Unimolecular Rate. The electron transfer reaction may be adiabatic, nonadiabatic, or somewhere in between.[44-48] A first-order quantum perturbation treatment of nonadiabatic electron transfer reactions yields the familiar result[3-5,47-49]

$$k(r) = \frac{2\pi}{\hbar}|V(r)|^2(\text{FC}) \qquad (11)$$

In eq 11 $V(r)$ is the matrix element between the reactant and product electronic states of the perturbation that gives rise to electron transfer. The quantity FC is a thermally weighted sum of Franck–Condon factors given by eq 12

$$\text{FC} = \frac{1}{Q}\sum_{i,f} e^{-E_i/k_BT}|\langle i|f\rangle|^2\delta(E_f - E_i + \Delta E) \qquad (12)$$

and has dimensions of (energy)$^{-1}$. In eq 12 i and f designate initial and final (reactants' and products') nuclear configuration states. The reactant state includes the pair of reactant molecules and the solvent surrounding them. Q is the nuclear partition function of the initial state. The functions $|i\rangle$ and $|f\rangle$ will be treated, for simplicity, in the harmonic oscillator approximation in the case of the intramolecular vibrations.

In the classical limit $\hbar\omega/k_BT \to 0$, and when frequency changes in individual vibrational modes are neglected, the FC given in eq 12 reduces to the expression in eq 13.[4,5,48]

$$\text{FC} = (4\pi\lambda k_BT)^{-1/2}\exp[-(\Delta E + \lambda)^2/(4\lambda k_BT)] \qquad (13)$$

As has been discussed elsewhere, e.g., ref 50, the quantum nonadiabatic result eq 11 and 12 plus a dynamical (harmonic oscillator)[47,51] assumption for the motion of the solvent does not allow for any large entropies of reaction.[52] To avoid this difficulty one can use, instead, a more nearly correct treatment of the polar solvent, one which is classical but in which no harmonic oscillations for the solvent are assumed.[44] In this case the Franck–Condon factor for the solvent is (cf. ref 5)

$$(\text{FC})_{\text{solv}} = (4\pi\lambda_{\text{out}}k_BT)^{-1/2}\exp[-(\Delta G^0 + E_f^v - E_i^v + \lambda_{\text{out}})^2/(4\lambda_{\text{out}}k_BT)] \qquad (14)$$

where the v superscripts denote vibrational energy. Equation 14 may be compared with the quantum results that we obtained in ref 50, where a quantum treatment of the solvent water was used, described by two modes which have frequencies of 1 and 170 cm^{-1}. The latter correspond to significant declines in the real part of the dielectric constant of water at those frequencies.[53,54] The 1-cm^{-1} mode was treated classically and the 170-cm^{-1} quantum mechanically.[50] The quantum $(\text{FC})_{\text{solv}}$ at room temperature was only 20% different from the classical value given by eq 14, and so in the present paper we shall use eq 14 for the solvent contribution.

We turn next to the estimate of $V(r)$. An adiabatic model corresponding to the nonadiabatic model of eq 13 yields

$$k_{\text{ad}} = \nu\exp[-(\Delta E + \lambda)^2/(4\lambda k_BT)] \qquad (15)$$

(cf. ref 44 with ΔG^0 replaced by ΔE). In eq 15 ν is a typical frequency for nuclear rearrangement, $\nu \sim 10^{13}$ s^{-1}. If one assumes at first that at some distance, e.g., at van der Waals' contact ($r = \sigma$), the reaction is adiabatic and that it becomes nonadiabatic for larger r's,[25] one can then evaluate the preexponential factor in eq 11–13 approximately by matching eq 11–13 with eq 15 at $r = \sigma$. Thereby expression 16 is obtained when this joining is made at r

$$(2\pi/\hbar)|V(\sigma)|^2(4\pi\lambda k_BT)^{-1/2} \sim 10^{13}\ \text{s}^{-1} \qquad (16)$$

$= \sigma$. For a reaction for which the nuclear reorganization energy term λ is 70 kJ/mol, the $V(\sigma)$ calculated from expression 16 is about 0.023 eV. If instead of expression 16 the reaction is nonadiabatic at $r = \sigma$, the actual value of $V(\sigma)$ is less than this, and we explore this possibility. Also, a more elaborate calculation a Landau–Zener-type theory for the adiabatic–nonadiabatic aspect could have been included.

For an exponential dependence of the matrix element on r, $V(r)$ is given by

$$|V(r)|^2 = |V(\sigma)|^2\exp[-\alpha(r - \sigma)] \qquad (17)$$

where $r - \sigma$ is on the average (and, for spherically symmetric reactants, exactly) the edge-to-edge distance between the reactants. The theoretically estimated[55,56] or experimentally inferred[57] values of α range from 2.6 to 1.1 Å^{-1}. The value of 2.6 refers to a theoretical calculation where the electron tunnels from one reactant to the other via a vacuum.[55] When medium is present, a value of 1.44 Å^{-1} was roughly estimated,[56] using a calculation based on an electron tunneling through a square barrier of about 2 eV.[58] More recent but ab initio calculations have been

(44) R. A. Marcus, *Annu. Rev. Phys. Chem.*, 15, 155 (1964); R. A. Marcus, *J. Chem. Phys.*, 24, 966 (1956); R. A. Marcus, *ibid.*, 43, 679 (1965).
(45) See P. P. Schmidt, *Electrochemistry*, 5, 21 (1975) for review.
(46) See ref 12 for review.
(47) V. G. Levich in "Physical Chemistry: An Advanced Treatise", Vol. 9B, H. Eyring, D. Henderson, and W. Jost, Eds., Academic Press, New York, 1970.
(48) V. G. Levich and R. R. Dogonadze, *Collect. Czech. Chem. Commun.*, 26, 193 (1961).
(49) R. R. Dogonadze, A. M. Kuznetsov, and M. A. Vorotyntsev, *Phys. Status Solidi B*, 54, 125, 425 (1972).
(50) P. Siders and R. A. Marcus, *J. Am. Chem. Soc.*, 103, 741 (1981).
(51) R. R. Dogonadze, A. M. Kuznetsov, and A. A. Chernenko, *Russ. Chem. Rev. (Engl. Transl.)*, 34, 759 (1965).
(52) The entropy of reaction that is treated by the nonadiabatic formula, eq 11 and 12, arises, in the harmonic oscillator approximation, from any noncanceling changes in the vibration frequencies that typically occur in oxidation–reductions. However, the inner-sphere contribution to ΔS^0 is usually minor, and for the polar solvent no changes in frequency are used.[47,50,51] The actual ΔS^0 is in large part due to reorganization of the solvent molecules, and this effect (e.g., reflected in electrostriction) is neglected in the harmonic oscillator treatment of the solvent (with fixed ionic radii). Because of the low frequencies involved, solvent reorganization can to a good approximation be treated classically at ordinary temperatures. The correct classical treatment of the solvent can be recovered simply by replacing ΔE with ΔG^0 in eq 12 when summing over the solvent modes. This is equivalent to the procedure used by Ulstrup and Jortner,[4] who use the classical expression[44] for the relevant Franck–Condon contribution.
(53) D. Draegert, N. Stone, B. Curnutte, and D. Williams, *J. Opt. Soc. Am.*, 56, 64 (1966).
(54) F. Franks, Ed., "Water: A Comprehensive Treatise", Vol. 1, Plenum Press, New York, 1972.
(55) J. Jortner, *J. Chem. Phys.*, 64, 4860 (1976).
(56) J. J. Hopfield, *Proc. Natl. Acad. Sci., U.S.A.*, 71, 3640 (1974).
(57) I. V. Alexandrov, R. F. Khairutdinov, and K. I. Zamaraev, *Chem. Phys.*, 32, 123 (1978).
(58) The familiar WKB formula (A. Messiah, "Quantum Mechanics", Vol. I, Wiley, New York, 1966, Chapter 6) for the probability of an electron of mass m tunneling from σ to r through a potential V, when E is the total energy of the electron, is $T \propto \exp[-(2/\hbar)\int_\sigma^r[2m(V(\rho) - E)]^{1/2}\,d\rho]$. If in the case of a nonadiabatic electron transfer $E - V(\rho)$ is taken to be roughly the binding energy B of the transferred electron, then $T \propto \exp[-2(2m_eB)^{1/2}(r - \sigma)/\hbar]$. Comparisons with eq 11 and 17 indicate $\alpha \simeq 2(2m_eB)^{1/2}/\hbar$. For $B = 2$ eV, this expression yields $\alpha = 1.5$ Å^{-1}.

given for the hexaaquoiron (II/III) self-exchange reaction ($\alpha \sim 1.8$ Å^{-1}).[59] (See also ref 60.) The 1.1 Å^{-1} was estimated indirectly from experiments on electron transfer between aromatic anions and aromatic molecules in frozen media.[57] (For a quite different system, reactions of solvated electrons in frozen media, values of α have also been estimated indirectly in the same manner.[16,61]) We shall use a value of 1.5 Å^{-1}. The results given later in Figures 1 and 2 are not very sensitive to the value of α. All calculations were performed with $T = 298$ K.

Method of Calculation. The equilibrium (no-reaction) steady-state solution to eq 6 is $g(r) = \exp[-U(r)/k_BT]$, when the two boundary conditions (i) $\lim g(r) = 1$ as $r \to \infty$ and (ii) eq 10 at $r = \sigma$ are employed. Reaction will cause deviation from this solution. If we rewrite the diffusion equation in terms of $h(r) = g(r) \exp(U/k_BT)$, then, at steady state ($\partial g/\partial t = 0$), eq 6 becomes

$$\frac{d}{dr}\left(r^2 e^{-U/k_BT}\frac{dh}{dr}\right) - \frac{r^2}{D}k(r)\, h(r) e^{-U/k_BT} = 0 \qquad (18)$$

The asymptotic solution to eq 18 at large r is obtained (for the case that U and k decrease more rapidly than $1/r$ at large r) by setting U and k equal to their values at large r, namely, zero, and then solving eq 18. This asymptotic solution is

$$h(r) \underset{r\to\infty}{\sim} 1 - c_2/r \qquad (19)$$

where c_2 is a constant and where we have satisfied the boundary condition that $h(r) \to 1$ as $r \to \infty$. We wish to construct the exact solution for $h(r)$ by numerical integration from $r = \sigma$ outward. Since $h(\sigma)$ is not known a priori, we first solve numerically for a function related to $h(r)$ by an unknown multiplicative constant c_1, $H(r) = c_1 h(r)$, and choose $H(\sigma)$ arbitrarily. ($H(\sigma) = 0.01$ was found to be convenient.) Equation 18 is first rewritten, in terms of $H(r)$, as an equivalent pair of coupled first-order differential equations to facilitate the numerical integration by a standard routine

$$\begin{aligned} d\theta/dr &= (r^2/D)k(r)e^{-U/k_BT}H \\ dH/dr &= r^{-2}e^{U/k_BT}\theta \end{aligned} \qquad (20)$$

where θ is defined by eq 21 and is $1/(4\pi D)$ times the flux

$$\theta = r^2 \exp(-U/k_BT)(dH/dr) \qquad (21)$$

at r. The boundary conditions at $r = \sigma$ are $H(\sigma) = 0.01$ and, from eq 10 and 21, $\theta(\sigma) = 0$. The numerical integration was begun at $r = \sigma$, and a standard program[62] for integration of a system of ordinary differential equations was used. $H(r)$ was calculated at successively larger values of r, using $k(r)$ as described in the preceding section, until it was found that $H(r)$ displayed its asymptotic behavior, that is, until $H(r)$ behaved as $c_1(1 - c_2/r)$ to within a small tolerance (constancy of c_1 and c_2 to 10^{-8}). At that point the calculation was stopped. The values of c_1 and c_2 were obtained from these parameters in $H(r)$ at large r, and $g(r)$ was computed by using

$$g(r) = H(r) \exp(-U(r)/k_BT)/c_1 \qquad (22)$$

Finally, k_{obsd} was calculated from the net flux at large r

$$k_{obsd} = 4\pi D \lim_{r\to\infty} [r^2\, dg/dr] = 4\pi D c_2 \qquad (23)$$

(An alternative way of calculating k_{obsd} is by integration of eq 4 using the numerically calculated $g(r)$, but this second method required smaller step sizes and tolerances to obtain convergence.)

Had $U(r)$ decreased as $1/r$ at large r, as for example for an unshielded Coulombic interaction potential, a related functional form for the asymptotic solution eq 19 and for the flux in eq 23 would have been used, $g(r) \sim c\{\exp[-U(r)/k_BT] - 1\} + 1$.

Steady-State Results

With $k(r)$ determined as described previously, we are in a position to examine numerically the effect on k_{obsd} of a reaction rate constant contributed from a range of internuclear separation distances. The steady-state (long-time) solutions of eq 4 and 6 will be examined first, since they are more easily found and correspond to existing experimental measurements.

The detailed calculations presented in this section are for the quenching of bipyridyl complexes of Ru(II) by various metal(III) bipyridyl complexes, studied experimentally by Creutz and Sutin.[14] The inner-sphere λ is estimated to be 15.5 kJ/mol and is associated with a frequency of 1300 cm^{-1}.[7] The outer-sphere λ has been estimated to be 54 kJ/mol.[63] If we calculate $k(r)$ as described in the preceding section (with $\alpha = 1.5$ Å^{-1} and $V(\sigma) = 0.023$ eV), we find that the k_{act} calculated from eq 5 at $\Delta G^0 = 0$ is 1.2×10^{10} M^{-1} s^{-1}, much higher than the currently estimated experimental value, $\sim 4 \times 10^8$ M^{-1} s^{-1}, for k_{obsd} (Appendix C). To obtain a k_{obsd} at $\Delta G^0 = 0$ in agreement with this value, one requires either a smaller $V(\sigma)$, a larger λ, or a less shielded repulsive potential $U(r)$. Use of $V(\sigma) \sim 0.0045$ eV gives a $k_{obsd}^{calcd} \sim 4 \times 10^8$ M^{-1} s^{-1} at $\Delta G^0 = 0$, and we report calculations with this $V(\sigma)$. Use, instead, of a larger $U(\sigma)$ but a $V(\sigma) = 0.023$ eV would have given similar results. For comparison we also report results obtained by using a larger λ and $V(\sigma) = 0.023$ eV.

The encounter distance, σ, has been estimated to be 14 Å,[63] and the experimental diffusion-limited rate constant is 3.5×10^9 M^{-1} s^{-1} at 298 K.[14] The quenching experiments were performed in 0.5 M sulfuric acid. Using the acid dissociation constant of 0.012 M for HSO_4^-,[64] we estimate the ionic strength to be 0.52 M. This large ionic strength implies a short Debye length, 4.2 Å, which in view of the large size of the reactants is expected to make the effect of Coulombic repulsion between the reactants small.

Numerical solution of eq 6 and comparison of these calculated k_{obsd} values with the maximum experimental value for k_{obsd} for the present system shows that with $\alpha = 1.5$ Å^{-1} and $V(\sigma) = 0.0045$ eV, $D = 3.0 \times 10^{-6}$ cm^2 s^{-1}. For ferric and ferrous trisphenanthroline complexes indirect approximate experimental (electrochemical) diffusion coefficients have been reported as 1.9×10^{-6} and 3.7×10^{-6} cm^2 s^{-1},[65] respectively, and so the value of D used in this paper (the sum of D's of the two tris(bipyridyl) complexes) is more or less consistent with these.

(59) M. D. Newton, *Int. J. Quantum Chem., Quantum Chem. Symp.*, 14, 363 (1980).
(60) S. P. Dolin, R. R. Dogonadze, and E. D. German, *J. Chem. Soc., Faraday Trans. 1*, 73, 648 (1977); S. U. M. Khan, P. Wright, and J. O'M. Bockris, *Sov. Electrochem. (Engl. Transl.)*, 13, 774 (1977).
(61) K. I. Zamaraev, R. F. Khairutdinov, and J. R. Miller, *Kinet. Katal.*, 21, 616 (1980); *Kinet. Catal. (Engl. Transl.)*, 21, 448 (1980).
(62) M. K. Gordon, Sandia Laboratories Report, SAND75-0211. For a discussion of the algorithm, see L. F. Shampine and M. K. Gordon, "Computer Solution of Ordinary Differential Equations", W. H. Freeman, San Francisco, CA, 1975.
(63) N. Sutin in "Tunneling in Biological Systems", B. Chance, D. C. Devault, H. Frauenfelder, J. R. Schrieffer, N. Sutin, Eds., Academic Press, New York, 1979, p 201.
(64) R. C. Weast, Ed., "Handbook of Chemistry and Physics", 56th ed., CRC Press, Cleveland, OH, 1975.
(65) I. Ruff and M. Zimonyi, *Electrochim. Acta*, 18, 515 (1973).

TABLE I: Comparison of the Approximate and the More Rigorous Treatments of Diffusion

ΔG°, eV	k_{obsd}, M^{-1} s^{-1} exact[a]	approximate[b]
0.0	4.1×10^8	4.1×10^8
−0.5	3.3×10^9	3.4×10^9
−1.0	3.4×10^9	3.4×10^9
−1.5	1.9×10^9	1.9×10^9
−2.0	2.1×10^7	2.1×10^7

[a] Calculated by using eq 4 and 6 with $k(r)$ the same as that for the solid line in Figure 1. [b] Calculated by using eq 2 and 5 with $k_{diff} = 3.5 \times 10^9$ M^{-1} s^{-1}, and $k(r)$ the same as that for the solid line in Figure 1.

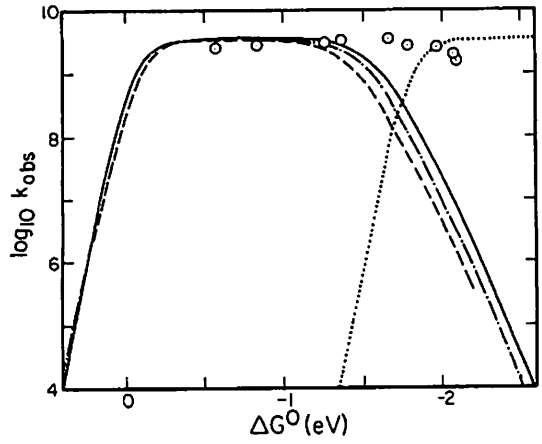

Figure 1. Calculated and experimental rates of electron-transfer quenching of ruthenium(II) bipyridyls vs. ΔG^0. The experimental points (circles) are due to Creutz and Sutin.[14,15] The solid line and dotted curves are for formation of ground-state products and an electronically excited product, respectively, using an r-dependent λ_{out}, with $\lambda_{out}(\sigma)$ = 54 kJ/mol and $V(\sigma)$ = 0.0045 eV. The dash–dot curve is for formation of ground-state products with λ_{out} fixed at $\lambda_{out}(\sigma)$. The dashed curve is the calculation reported in ref 7 in which reaction occurred only at $r = \sigma$.

Calculations were made for the formation of ground-state products and of an electronically excited $Ru^{III}bpy_3$ product, using the excitation energy, 1.76 eV, employed in ref 7.[66] The formation of alternative excited products is discussed in Appendix D. We have neglected any possible spin-restriction effects.

With the parameters discussed above and the $k(r)$ discussed in the preceding section, we have calculated the reactant pair distribution function $g(r)$ and the observed rate constant k_{obsd} as a function of ΔG^0. We first test the approximate eq 2 and 5, using for k_{diff} the maximum value observed for k_{obsd} (which we will call the "experimental" k_{diff}, since $k_{act}^{max} \gg k_{diff}$). In Table I the results from eq 2 and 5 are compared with those using the numerical steady-state solution of eq 4 and 6. The agreement is about 5% over the entire range of ΔG^0's studied, +0.6 to −3.0 eV. The D inferred from k_{obsd}^{max} ($\simeq k_{diff}$) when eq 3 is used was 3.5×10^{-6} cm^2 s^{-1}, which is close to the value (3.0×10^{-6}) inferred by using, instead, eq 4 and 6. Had the latter value been used instead of 3.5×10^{-6}, the agreement in Table I would have been about 10% instead of 5%.

(66) In the calculations for the formation of an electronically excited $Ru(bpy)_3^{3+}$ product, we have used the same $V(r)$ as we did for the calculations involving ground-electronic-state products. The lowest excited electronic state of $Ru(bpy)_3^{2+}$ is a metal-to-ligand charge-transfer state (see: ref 76; F. E. Lytle and D. M. Hercules, *J. Am. Chem. Soc.*, 91, 253 (1969); R. A. Palmer and T. S. Piper, *Inorg. Chem.*, 5, 864 (1966)), while the lowest excited electronic state of $Ru(bpy)_3^{3+}$ has been characterized as a ligand-to-metal charge-transfer state (B. Mayoh and P. Day, *Theor. Chim. Acta*, 49, 259 (1978); S. F. Mason, *Inorg. Chim. Acta, Rev.*, 2, 89 (1968)). Because of the nature of the Ru(II) and Ru(III) excited states, it might be appropriate to use a different $V(r)$ for ground-state and excited products, but the necessary data are lacking.

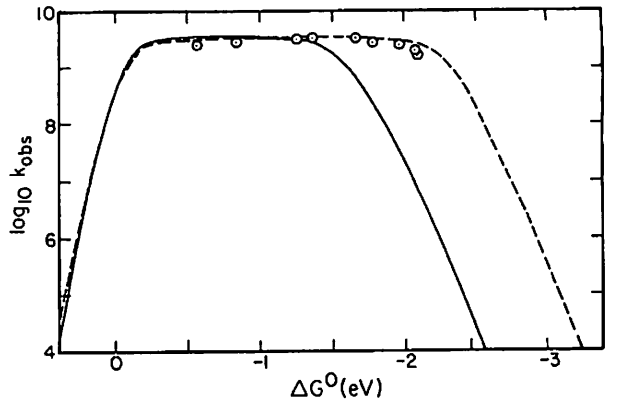

Figure 2. Calculated and experimental rates of electron-transfer quenching of ruthenium(II) bipyridyls vs. ΔG^0. The solid curve is taken from Figure 1. The dashed curve is with an r-dependent λ_{out}, $\lambda_{out}(\sigma)$ = 83 kJ/mol, and $V(\sigma)$ = 0.023 eV. The experimental points (circles) are those of Creutz and Sutin.[14,15]

The results for k_{obsd} vs. ΔG^0 are plotted in Figure 1, where the experimental points are indicated by circles. The solid line in this figure is the result of the present calculation using eq 4 and 6, and the dotted curve is for formation of an electronically excited Ru(III) product. For the dash–dot line the solvent reorganization energy was held constant at the value that it has when $r = \sigma$, rather than being allowed to vary with r as it should. The dashed line in Figure 1 is a result taken from ref 7, based on eq 2, and assumes that reaction occurs at the contact distance only. There, λ_{out} was taken to be $\lambda_{out}(\sigma)$ = 54 kJ/mol, and the experimental value of k_{diff} was introduced into eq 2.

The closeness of the solid and dash–dot curves in Figure 1 shows that the effect of having an r-dependent λ_{out} instead of a λ_{out} fixed at $r = \sigma$ is small. The approximation used in ref 1 of treating the reaction as occurring at $r = \sigma$ and as being adiabatic there agrees well with the present results (cf. solid and dash–dot curves in Figure 1), because of compensation. (The nonadiabaticity for the solid curve decreases the rate but the reaction over a distance causes an enhanced rate, compared with the rate for the dash–dot curve.)

To be consistent with the experimental data in Figure 1, if one uses the above λ's, it is necessary to introduce the formation of an electronically excited Ru(III) product, namely, the dotted curve there. The calculated total k_{obsd}, which is the sum of the calculated rate constants for forming ground- and excited-state products, then agrees with the experimental points to a factor of about 4.

If a larger value of λ_{out} or of λ_{in} were used, this remaining discrepancy could be reduced significantly.[15] For example, with $\lambda = \lambda_{out} + \lambda_{in}$ increased by only 5%, to 73 kJ/mol (and $V(\sigma)$ accordingly increased to 0.0054 eV to maintain agreement with the "experimental" rate constant at $\Delta G^0 = 0$), we find that the calculated total k_{obsd} agrees with the experimental points to within a factor of about 2.

In Figure 2 calculations having a larger but still r-dependent λ_{out} ($\lambda_{out}(\sigma)$ = 83 kJ/mol, $V(\sigma)$ = 0.023 eV) are given (dashed line) and compared with the solid line ($\lambda_{out}(\sigma)$ = 54 kJ/mol, $V(\sigma)$ = 0.0045 eV) of Figure 2. A slightly smaller D (2.6×10^{-6} cm^2 s^{-1}) was required to make the larger λ_{out} calculation yield the experimental value of the maximum k_{obsd}, 3.5×10^9 M^{-1} s^{-1}.

The position of the dashed curve in Figure 2 in the inverted region relative to the other curve reflects the large value for λ_{out} in that case (≥83 kJ/mol). The value of λ_{out} for the solid curve was ≥54 kJ/mol. As is evident from

the approximate eq 14, the greater λ_{out} the less the tendency to inversion, other things being equal. Indeed, one sees from Figure 2 that, if $\lambda_{out}(\sigma)$ equalled 83 kJ/mol, it would not be necessary to invoke the excited electronic state of Ru(III).

Short-Time Experiments

Reactions that are fast relative to diffusion are controlled by the rate of diffusion rather than by their "activated" rates, and so diffusion can mask interesting rate behavior. In the case of reactions that can be induced in a very short time, for example, by a pulse of light, such as reaction 24, followed by reaction 25, this masking effect may be reduced. In a fast bimolecular reaction 25 in which the

$$red_2 + h\nu \rightarrow red_2^* \quad (24)$$

$$ox_1 + red_2^* \rightarrow red_1 + ox_2 \quad (25)$$

reactants ox_1 and red_2^* are initially randomly distributed, reaction causes the reactant pair distribution function, $g(r,t)$, to depart from its equilibrium value. Since the reactants closest together tend to react first, $g(r,t)$ becomes increasingly depleted near $r = \sigma$ as time increases. At long time $g(r,t)$ approaches the steady-state distribution function discussed previously. However, at small t, the distribution of reactants is closer to the equilibrium one, even for quite fast reactions, and the observed rate constant is then nearer the value that it would have in the limit of infinitely rapid diffusion. That is, as $t \rightarrow 0$, k_{obsd} approaches the activated rate constant k_{act} given by eq 5. Thus, if the rates of fast reactions such as reaction 25 can be measured at sufficiently short times, the masking effect of diffusion can be circumvented.

For simplicity of presentation, we shall consider first the time-dependent problem for the case that $U = 0$, a realistic case at the present high ionic strength. The following time-dependent solution to eq 4 and 6 with $U = 0$ is well-known and will suffice to provide order-of-magnitude estimates for the rate enhancement to be expected at short times. When reaction occurs only at a fixed internuclear separation σ, with bimolecular rate constant k_{act}, and in the absence of long-range forces between the reactants, k_{obsd} is given by[34,67]

$$k_{obsd}(t) = \frac{1}{1/k_{act} + 1/k_{diff}}\left[1 + \frac{k_{act}}{k_{diff}} e^{x^2} \text{erfc}\,(x)\right] \quad (26)$$

where erfc (x) is the well-known complementary error function

$$\text{erfc}\,(x) = (2/\sqrt{\pi}) \int_x^\infty e^{-u^2}\, du \quad (27)$$

$$x = (Dt)^{1/2}(1 + k_{act}/k_{diff})/\sigma \quad (28)$$

and k_{act} is for reaction occurring at $r = \sigma$, but we shall use (cf. Appendix B for the steady-state case)

$$k_{act} = 4\pi \int_\sigma^\infty k(r) r^2\, dr \quad (29)$$

D is again the sum of the reactants' diffusion coefficients. k_{diff} is the diffusion-limited rate constant and is the same as in eq 3, but with $U = 0$, i.e.

$$k_{diff} = 4\pi D\sigma \quad (30)$$

In obtaining eq 26 the usual boundary condition,[67] eq 31, on the flux at $r = \sigma$, was satisfied.

$$4\pi D\sigma[\partial g(\sigma)/\partial \sigma] = k_{act}\, g(\sigma) \quad (31)$$

(67) F. C. Collins and G. Kimball, *J. Colloid Sci.*, 4, 425 (1949).

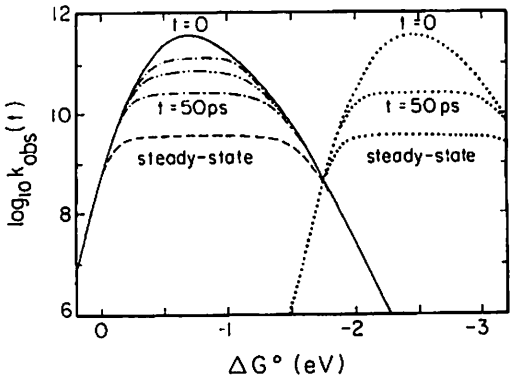

Figure 3. Observed rate constant at various times following the onset of reaction. The values of k_{obsd} are calculated from eq 26. Observation times: (-·-) 1 and (-···-) 5 ps. The $k_{obsd}(t)$ for formation of an excited-state Ru(III) is depicted by the dotted lines.

At large t the second term in the brackets in eq 26 vanishes, so that eq 26 reduces to the steady-state expression, eq 2. As $t \rightarrow 0$, on the other hand, k_{obsd} as given by eq 26 approaches k_{act}. The rate behavior for large values of k_{act} at sufficiently short times is, thus, not masked by diffusion.

Figure 3 shows the behavior of k_{obsd} predicted by eq 26 at various times from $t = 0$ to $t = 1$ μs. The time $t = 1$ μs is sufficiently long that a steady state has been reached. In making the calculation for Figure 3, k_{act} was calculated with eq 29, using $k(r)$ as described in the preceding section. The experimental value of k_{diff}, 3.5×10^9 M^{-1} s^{-1}, was used. At observation times on the order of 0.5 ps, which may be accessible by using present subpicosecond techniques, the rate constants are greatly enhanced, and there is a pronounced double maximum in the plot in Figure 3, and also, indeed, for the 5- and 50-ps curves. An experimental study at small times would be desirable and may in fact distinguish the behavior in Figure 2 from that in Figure 3. Calculations using the time-dependent counterpart of the present treatment would be somewhat more accurate than the results given in Figure 3.

A solution analogous to eq 26 but which allows for a general nonzero $U(r)$ is also available.[68] With $U(r)$ as described in a preceding section, k_{act} as defined in eq 5, and $k_{diff} = 3.5 \times 10^9$ M^{-1} s^{-1}, the rate constants were calculated by using the equation given in ref 68. As expected at the present high ionic strength, the recalculated values differ little from those presented in Figure 3.

It may, of course, be equally useful or more useful to look experimentally for inverted behavior in electron transfer reactions between redox centers that are linked chemically (cf. ref 69). Having the reactants linked together would entirely circumvent the problem of slow diffusion. Also, if the chemical link were rigid, the reaction would be forced to occur at a single, well-defined reactant separation distance.

We consider the first-order reaction shown in reactions 32 and 33. Reaction 33 would be followed by the reverse

$$ox_1\sim\sim red_2 + h\nu \rightarrow ox_1\sim\sim red_2^* \quad (32)$$

$$ox_1\sim\sim red_2^* \rightarrow red_1\sim\sim ox_2 \quad (33)$$

electron transfer to reform ox_1 and red_2. In reactions 32 and 33 the oxidized and reduced species have been linked by some bridging group(s). For the case of a $\lambda_{out}(\sigma) = 54$ kJ/mol, i.e., for two reactants virtually in contact, the

(68) M. R. Flannery, *Phys. Rev. Lett.*, 47, 163 (1981).

(69) J. C. Curtis, J. S. Bernstein, R. H. Schmehl, and T. J. Meyer, *Chem. Phys. Lett.*, 81, 48 (1981).

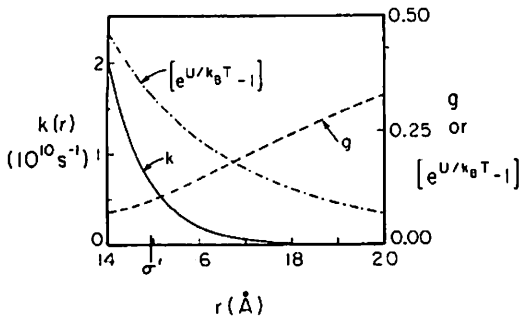

Figure 4. Behavior of $k(r)$, $g(r)$, and $\exp[U(r)/k_BT]$ as a function of r. The calculations are given for the conditions given by the solid line in Figure 1 at $\Delta G^0 = -1.3$ eV. $g(r)$ rises to 0.5 at $r \cong 26$ Å and eventually approaches unity.

results for the rate constant k are given by the $t = 0$ plot in Figure 3, apart from absolute scale.

Finally, it remains to consider the relationship mentioned earlier between the charge-transfer absorption spectrum vs. frequency plot and the ln k_{act} vs. ΔG^0 plot. We do so in the next section.

Analogy between Charge-Transfer Spectrum and Plot of k_{act} vs. ΔG^0

The probability of the optical dipole-induced transition from the ith vibrational level of electronic state $|a\rangle$ to the fth vibrational level of electronic state $|b\rangle$ is given by[4]

$$\Gamma(\Delta E_1 \pm h\nu) = C \sum_{i,f} e^{-E_i/k_BT}|\langle i|f\rangle|^2\delta[E_f - E_i + (\Delta E_1 \pm h\nu)] \quad (34)$$

using the Golden Rule and the Condon approximations. In eq 34, C is a proportionality constant $(2\pi|\langle a|\mu|b\rangle|^2/Q\hbar)$, ΔE_1 is the difference in energy of the zero-point vibrational levels of electronic states $|b\rangle$ and $|a\rangle$ for a particular system, and $h\nu$ is the energy of the radiation emitted (+) or absorbed (−). E_f and E_i are the vibrational energies associated with $|f\rangle$ and $|i\rangle$.

Comparing eq 34 with eq 11 and 12, we see that Γ/C is the same function of $\Delta E_1 \pm h\nu$ that k_{act}/C' is of ΔE, where $C' = 2\pi|V(r)|^2/Q\hbar$. Thus, since Γ, and hence Γ/C, has a maximum as a function of $\Delta E_1 \pm h\nu$ (where this argument is varied by varying $h\nu$) in the absorption plot, k_{act} must have a maximum as a function of ΔE. In the k_{act} vs. ΔE plot, ΔE is varied by studying a series of reactants, by varying one of the reactants, in which (ideally) the vibration frequencies and bond lengths of this series of reactants are fixed, as are those of the corresponding products, and so the ψ_i's, ψ_f's, E_i's, and E_f's are the same for each member of the series. ΔE is the only variable in this series. Because of the constancy of the ψ_i's, etc., the ΔS^0 is also a constant, and so a plot of k_{act} vs. ΔE is merely a displacement of the plot of k_{act} vs. ΔG^0. In summary, the maximum in the absorption coefficient vs. absorption frequency plot, well-known in charge-transfer (and other) absorption spectra, implies a maximum in the plot of k_{act} vs. ΔG^0. The condition on the argument is that eq 34 provide a suitable description of the former and that eq 11 and 12 adequately describe the latter.

Conclusion

We have seen that the r dependence of the solvent reorganization energy increases the predicted rate constant in the inverted region, as expected. For the particular system for which calculations were performed, the increase was relatively small.

In the calculation of steady-state rate constants, we found it adequate to use a simple analytical approximation to the problem, eq 2, in which one calculates an activated rate constant and then obtains the observed rate constant as the harmonic mean of the activated and diffusion-limited rate constants.

It is suggested that experiments measuring the rate of electron transfer at very short times following the onset of reaction can improve the chances of observing inverted behavior that may be masked by the slowness of diffusion in typical steady-state measurements. It may also be fruitful to seek inverted behavior in electron transfer reactions between chemically linked redox centers.

Acknowledgment. It is a pleasure to acknowledge support of this research by a grant from the National Science Foundation. The calculations reported in this paper made use of the Dreyfus–NSF theoretical chemistry computer which was funded through grants from the Camille and Henry Dreyfus Foundation, the National Science Foundation, and the Sloan Fund of the California Institute of Technology.

Appendix A

Comment on Eq 7. The approximations contained in eq 7 include the following: (1) replacing the discrete molecular environment of the ion, namely, the solvent and the counterions, by a dielectric continuum and a continuous charge distribution, (2) use of the linearized form of this continuum (Poisson–Boltzmann) equation, eq A1, (3) treating the reactants as spherical even in cases where they are not, and (4) neglecting dielectric image effects arising from the presence of a low dielectric constant sphere (the second ion) in the presence of the first, e.g., by using as a solution eq A2.

The linearized Poisson–Boltzmann equation for the electrostatic potential ψ is

$$\nabla^2\psi = \kappa^2\psi \quad (A1)$$

When there are two central ions of charges $\gamma z_1 e$ and $\gamma z_2 e$ (γ is a charging parameter which will later be increased from 0 to 1), eq A1 has the approximate solution at any point in the medium

$$\psi = \frac{\gamma z_1 e e^{\kappa a_1} e^{-\kappa R_1}}{(1 + \kappa a_1)\epsilon R_1} + \frac{\gamma z_2 e e^{\kappa a_2} e^{-\kappa R_2}}{(1 + \kappa a_2)\epsilon R_2} \quad (A2)$$

where a_i is given by eq 8 and R_i is the distance from the point to the center of ion i. Equation A2 is the sum of potentials that one would have if only one of the two central ions were present, individual solutions which are well-known.[42a] Equation A2 ignores the fact that, when one brings ion 2 up to ion 1, one is changing the boundary in the vicinity of ion 1 (a new boundary is introduced). Accordingly, the first term, which formerly was an exact solution to eq A1, is now only approximate; analogous remarks apply to the second term.

The potential energy of interaction of the two central ions, $U(r)$ in eq 7, is obtained by multiplying the second term in eq A2 by the infinitesimal element of charge $z_1 e\, d\gamma$, replacing R_2 by its average value r at the center of ion 1 (an approximation, which we shall eliminate in a later paper) and multiplying the first term in eq A2 by $z_2 e\, d\gamma$, replacing R_1 by its average value r at the center of ion 2, and integrating γ from 0 to 1. The missing terms, e.g., the first term in eq A2 times $z_1 e\, d\gamma$, contribute to the interaction of ion 1 with its environment and so are present at $r = \infty$. Therefore, they do not contribute to the mutual interaction energy of ions 1 and 2. The integration yields eq 7.

Another expression for $U(r)$ which has sometimes been used, for the case of a large ion (ion 1) interacting with a

small one, is[70a] (cf. ref 70b)

$$U(r) = \psi(r, \text{ion 1 only present})z_2e \qquad \text{(A3)}$$

(For the case of a spherical charge distribution on ion 1, this $U(r)$ is $z_1z_2e^2 \exp[\kappa(a_1 - r)]/[\epsilon r(1 + \kappa a_1)]$.) This expression and eq 7 yield the same answer in several limiting cases: (a) $a_1 = 0$, $a_2 = 0$, (b) $a_1 = a_2$, and (c) $\kappa = 0$. Equation A3 is commonly also tacitly used for the interaction of an ion (ion 2) with an electrode (ion 1 is allowed to become extremely large, and hence ultimately a plane). In the present case, the two radii a_1 and a_2 are equal, and so eq 7 and A3 both yield the same result, namely, eq 9.

Appendix B

Derivation of Eq 2 for Reactions over a Range of r's. We obtain eq 5 first: If diffusion is sufficiently fast, the steady-state solution to eq 6 is given by the equilibrium expression

$$g(r) = \exp[-U(r)/k_BT] \qquad \text{(fast diffusion)} \quad \text{(B1)}$$

for $r \geq \sigma$, and $g(r \leq \sigma) = 0$. The activated bimolecular rate constant may be obtained by substituting this equilibrium g into eq 4, yielding eq 5.

To obtain an approximate steady-state solution[25] of eq 6 under other conditions, the equation is first rewritten as

$$\frac{D}{r^2}\frac{d}{dr}\left[e^{-U/k_BT}r^2\frac{d}{dr}(ge^{U/k_BT})\right] = k(r)\,g(r) \qquad \text{(B2)}$$

Integration yields

$$De^{-U/k_BT}r^2\frac{d}{dr}(ge^{U/k_BT})|_{r=\sigma}^{R} = \int_\sigma^R k(r)\,g(r)r^2\,dr \qquad \text{(B3)}$$

The flux is given by $4\pi r^2D$ times the left-hand side of eq 10, and so the left-hand side of eq B3 is $1/4\pi$ times the flux at $r = R$ minus that at $r = \sigma$. The condition of zero net flux across the $r = \sigma$ boundary (eq 10) implies that in the left-hand side of eq B3 the term at the lower limit $r = \sigma$ vanishes. The unimolecular rate constant $k(r)$ is, as discussed in the text, a rapidly decreasing function of r. For r greater than some distance σ', where $\sigma' - \sigma$ is a small quantity, $k(r)$ is essentially zero. Therefore, for $R > \sigma'$ the right-hand side of eq B3 may be approximately replaced by its limit at $R \to \infty$, and, because of the vanishing of the left-hand side of eq B3 at its lower limit, we then have (writing r instead of R)

$$De^{-U/k_BT}r^2\frac{d}{dr}(ge^{U/k_BT}) = \int_\sigma^\infty k(r)\,g(r)r^2\,dr \qquad (r > \sigma') \qquad \text{(B4)}$$

Substituting eq 4 for the integral over r into eq B4 allows one to rewrite the latter as

$$De^{-U/k_BT}r^2\frac{d}{dr}(ge^{U/k_BT}) = k_{obsd}/4\pi \qquad (r > \sigma') \quad \text{(B5)}$$

Rearranging eq B5 and integrating from σ' to ∞ yields

$$\frac{k_{obsd}}{4\pi D}\int_{\sigma'}^\infty e^{U/k_BT}\frac{dr}{r^2} = [g(r)e^{U/k_BT}]|_{r=\sigma'}^{\infty} \qquad \text{(B6)}$$

The potential $U(r)$ vanishes, by definition, as $r \to \infty$, and we require $\lim g(r) = 1$ as $r \to \infty$. Thus, we obtain

$$k_{obsd}/k'_{diff} = 1 - g(\sigma')\exp[U(\sigma')/k_BT] \qquad \text{(B7)}$$

where

$$k'_{diff} = 4\pi D/\int_{\sigma'}^\infty e^{U/k_BT}r^{-2}\,dr \qquad \text{(B8)}$$

We now proceed to evaluate the second term in the right-hand side of eq B7 in terms of the activation-controlled rate constant k_{act}. If the product $\exp[U(r)/k_BT]g(r)$ varies only slowly for $\sigma < r < \sigma'$, then k_{obsd} is given (using eq 4) approximately by

$$k_{obsd} \simeq 4\pi g(\sigma')e^{U(\sigma')/k_BT}\int_\sigma^\infty k(r)r^2e^{-U(r)/k_BT}\,dr \qquad \text{(B9)}$$

which, using eq 5, becomes

$$g(\sigma')\exp[U(\sigma')/k_BT] \simeq k_{obsd}/k_{act} \qquad \text{(B10)}$$

If we substitute eq B10 into eq B7, we obtain

$$k_{obsd}/k'_{diff} \simeq 1 - k_{obsd}/k_{act} \qquad \text{(B11)}$$

Because $\sigma' - \sigma$ is a small quantity, k'_{diff} is approximately equal to k_{diff}, where k_{diff} is defined as in eq B8, but with σ in place of σ'. Substituting k_{diff} for k'_{diff} in eq B11 and rearranging yields eq 2.

Finally, in Figure 4, to illustrate how much or little $g(r)\exp[U(r)/k_BT]$ varies in the interval $\sigma' - \sigma$, we plot $k(r)$, $g(r)$, and $\exp[U(r)/k_BT]$ vs. r, for $\Delta G^0 = -1.3$ eV. The quantity σ' is indicated approximately, chosen so that $k(\sigma') = k(\sigma)/3$. The unimolecular rate constant $k(r)$ was calculated in the same way as for the solid line in Figure 1. From the results in Figure 4, the product $g(r)\exp[-U(r)/k_BT]$ varies by ~20% over the interval $\sigma < r < \sigma'$. A similarly small change is observed with other values of ΔG^0. This observation suggests that it is adequate to treat $g(r)\exp[U(r)/k_BT]$ as constant for $\sigma < r < \sigma'$.

Appendix C

"Experimental" Rate Constant of the Reaction of $Ru^{II}(bpy)_3^*$ with $M^{III}(bpy)_3$. The "experimental" rate constant given in the text for reaction C3 at $\Delta G^0 = 0$ is ~4 × 10^8 M^{-1} s^{-1}. To obtain this value, we make use of the self-exchange rate constant (~10^8 M^{-1} s^{-1}) estimated[71] for reaction C1 and that estimated for reaction C2, 1.2 × 10^9

$$Ru^{II}bpy_3^* + Ru^{III}bpy_3 \rightarrow Ru^{III}bpy_3 + Ru^{II}bpy_3^* \qquad \text{(C1)}$$

M^{-1} s^{-1}.[72] The latter was k_{obsd} for the oxidation of $Ru(bpy)_3^{2+}$ by $Ru(phen)_3^{3+}$, for which $\Delta G^0 \simeq 0.01$ eV.

$$Ru^{II}bpy_3 + Ru^{III}bpy_3 \rightarrow Ru^{III}bpy_3 + Ru^{II}bpy_3 \qquad \text{(C2)}$$

Corrected for diffusion by using eq 2, the activation rate constant k_{act} for eq C2 is about 2 × 10^9 M^{-1} s^{-1}.

The geometric mean of these activation rate constants is 4.5 × 10^8 M^{-1} s^{-1} and will be used for k_{act} for the reaction

$$Ru^{II}bpy_3^* + M^{III}bpy_3 \rightarrow Ru^{III}bpy_3 + M^{II}bpy_3 \qquad \text{(C3)}$$

at $\Delta G^0 = 0$. We use the cross relation[1,2] to estimate the rate constant for reaction C3 at $\Delta G^0 = 0$ as the geometric mean of the rate constants for reactions C1 and C2. Sutin has argued[73] that the cross relation should be applicable even for nonadiabatic reactions if the electronic matrix element $V(r)$ for reaction C3 is equal to the geometric mean of the matrix elements for reactions C1 and C2. Assuming that that condition is approximately satisfied, we find k_{act} = 4.5 × 10^8 M^{-1} s^{-1} for reaction C3 at $\Delta G^0 = 0$. Corrected for diffusion by using eq 2, this k_{act} yields a k_{obsd} for re-

(70) (a) J. W. van Leeuwen, F. J. M. Mofers, and E. C. I. Veerman, *Biochim. Biophys. Acta*, 635, 434 (1981), cf. eq 5; (b) W. H. Koppenol, C. A. J. Vroonland, and R. Braams, *ibid.*, 503, 499 (1978).

(71) C.-T. Lin, W. Bottcher, M. Chou, C. Creutz, and N. Sutin, *J. Am. Chem. Soc.*, 98, 6536 (1976).

(72) R. C. Young, F. R. Keene, and T. J. Meyer, *J. Am. Chem. Soc.*, 99, 2468 (1977).

(73) N. Sutin, *Acc. Chem. Res.*, 1, 225 (1968).

action C3 of $\sim 4 \times 10^8$ M^{-1} s^{-1}. Incidentally, the reaction

$$Cr^{III}mebpy_3^* + Ru^{II}bpy_3 \rightarrow Cr^{II}mebpy_3 + Ru^{III}bpy_3 \quad (C4)$$

in 1 M H_2SO_4 has a ΔG^0 very close to zero and has a k_{obsd} of $\sim 2 \times 10^8$ M^{-1} s^{-1}.[15]

Appendix D

Formation of Other Electronically Excited States. The possibility of forming other electronically excited products was also considered. Formation of an electronically excited Ru(II) product is thermodynamically less favorable by 0.3 eV[74,75] than formation of an excited Ru(III), so Ru(II) products were assumed to be formed in their ground electronic states. The excitation energy for formation of $Os(bpy)_3^{2+}$ is[76,77] 1.78 eV (similar to that for $Ru(bpy)_3^{2+}$, 1.76 eV), and associated with the excitation is an inner-sphere reorganization energy of about 2 kJ/mol ($^1/_8$ of the Stokes shift)[78] at a frequency of ~ 1300 cm^{-1} (the vibrational spacing observed in the low-temperature emission spectrum[76,78]). The formation of an electronically excited Os(II) product may be less favorable (or at least no more favorable) than formation of an excited Ru(III) product, depending on the assumptions.[79] Finally, although the excitation energy of $Cr(bpy)_3^{2+}$ is only about[80,81] 1.05 eV, which is lower than the Ru(III) excitation energy, the reactions to form the electronic ground state of the Cr(II) product already lie in the "normal" (i.e., not inverted) region, and so it would be less favorable to form an electronically excited Cr(II) product.

(74) G. Hager and G. Crosby, *J. Am. Chem. Soc.*, **97**, 7031 (1975).
(75) C.-T. Lin, W. Bottcher, M. Chou, C. Creutz, and N. Sutin, *J. Am. Chem. Soc.*, **98**, 6536 (1976).
(76) F. Zuloago and M. Kasha, *Photochem. Photobiol.*, **7**, 549 (1968).
(77) C.-T. Lin and N. Sutin, *J. Phys. Chem.*, **80**, 97 (1976).
(78) G. A. Crosby, D. M. Klassen, and S. L. Sabath, *Mol. Cryst.*, **1**, 453 (1966).
(79) E.g., if one assumes λ_{in} for formation of an excited Ru(III) product to be 15.5 kJ/mol, in the absence of specific knowledge to the contrary, while that for formation of an excited Os(II) product is 8 kJ/mol, and if one sets λ_{in} for formation of unexcited Ru(III) equal to[7] 15.5 kJ/mol, one calculates the rate of formation of excited Ru(III) and unexcited Os(II) to be 2.5 times faster than that of unexcited Ru(III) and excited Os(II). Throughout, a $\lambda_{out}^{(\sigma)} = 54$ kJ/mol, a $D = 3.0 \times 10^{-6}$ cm^2 s^{-1}, and a $\sigma = 14$ Å were used, together with the r-dependent λ_{out} and a given $V(r)$ ($V(\sigma) = 0.0045$ eV and $\alpha = 1.5$ $Å^{-1}$). $V(r)$ may, of course, differ for these reactions.
(80) E. Kõnig and S. Herzog, *J. Inorg. Nucl. Chem.*, **32**, 585 (1970).
(81) I. Fujita, T. Yazaki, Y. Torii, and H. Kobayashi, *Bull. Chem. Soc. Jpn.*, **45**, 2156 (1972).